Evidence of component merging equatorward of the cusp

Article

Published Version

www.reading.ac.uk/centaur

CentAUR

Central Archive at the University of Reading

Reading's research outputs online

Evidence of component merging equatorward of the cusp

M. O. Chandler,[1] S. A. Fuselier,[2] M. Lockwood,[3] and T. E. Moore[4]

Abstract. The Polar spacecraft passed through a region near the dayside magnetopause on May 29, 1996, at a geocentric distance of ~8 R_E and high, northern magnetic latitudes. The interplanetary magnetic field (IMF) was northward during the pass. Data from the Thermal Ion Dynamics Experiment revealed the existence of low-speed (~50 km s^{-1}) ion D-shaped distributions mixed with cold ions (~2 eV) over a period of 2.5 hours. These ions were traveling parallel to the magnetic field toward the Northern Hemisphere ionosphere and were convecting primarily eastward. The D-shaped distributions are distinct from a convecting Maxwellian and, along with the magnetic field direction, are taken as evidence that the spacecraft was inside the magnetosphere and not in the magnetosheath. Furthermore, the absence of ions in the antiparallel direction is taken as evidence that low-shear merging was occurring at a location southward of the spacecraft and equatorward of the Southern Hemisphere cusp. The cold ions were of ionospheric origin, with initially slow field-aligned speeds, which were accelerated upon reflection from the magnetopause. These observations provide significant new evidence consistent with component magnetic merging sites equatorward of the cusp for northward IMF.

1. Introduction

The interchange of mass and energy between the Sun and Earth by way of magnetic field line reconnection has been a subject of study for nearly 40 years. The original work of *Dungey* [1961] has been followed by substantial gains in both experimental and theoretical work. This work has led to confirmation of much of the original predictions. One of the more recent and useful tools for studying the nature of reconnection at the magnetopause is ion and electron velocity-space distributions. The constant improvements in detector resolution and sensitivity and the number of different locations in geospace in which they have been placed have made it possible to distinguish clearly the different components in mixed plasma populations and to relate these populations to their region of origin. Thus detailed observations of all components of the plasma that have been affected by the reconnection processes allow for reconstruction of the basic field line topology for specific events and conditions.

While much attention has been given to the "classic" antiparallel merging that occurs during periods of southward directed (when referenced to the GSM coordinate system) interplanetary magnetic field (IMF), the conditions under which merging can occur during periods of northward directed IMF (NBZ) have only recently been studied [e.g., *Onsager and Fuselier*, 1994; *Fuselier et al.*, 1995, 1997]. Such conditions lead to expectations of merging poleward of the cusp in both the Northern and Southern Hemispheres as well as equatorward of the cusp. The different

possibilities will result in distinctly different plasma populations being observable from a given location. By studying ion data from within the dayside low-latitude boundary layer, *Onsager and Fuselier* [1994] showed that the location of the reconnection site was in the dayside equatorial plane. In later work, *Fuselier et al.* [1997] were able, using both electron and ion observations, to distinguish between reconnection sites in the lobe and those equatorward of the cusp for NBZ conditions.

The event of May 29, 1996, possessed the proper conditions for so-called low magnetic shear merging. Measurement of the ion and electron populations and the magnetic and electric field were made as the Polar spacecraft passed through the dayside magnetosphere at ~8 R_E geocentric distance. In particular, the core ion measurements of the Thermal Ion Dynamics Experiment (TIDE) provided sufficient detail to allow the reconnection site to be determined as well as the resultant field line topology.

2. Observations

The TIDE ion sensor is designed to provide nearly three-dimensional (only 0°–157.5° coverage with respect to the spin axis) measurements of core ions in the energy range 0.3–450 eV above spacecraft potential in one 6 s satellite spin period [*Moore et al.*, 1995]. Two sources of noise are present in this data, both due to solar UV. One source is due to entry of reflected sunlight into the instrument apertures, which results in spurious H$^+$ and O$^+$ signals. The second is due to sunlight entering the instrument through an unknown location and results in a general background signal. Both sources occur at specific spin-phase angles and are subtracted using a background signal generated every other day from in-flight data. An additional noise source that results in a general enhancement of the noise counts results from energetic particles. Noise of this type that occurs evenly across all masses and energies can be accounted for by looking for a distribution in phase space density, which has an E^{-2} form. In this study, one-dimensional slices of the distribution function have had such noise removed by eliminating data that falls below a constant n-count level. The value of n is chosen depending on the number of samples that are averaged. For all cases shown, 10 samples

---

[1] Space Sciences Laboratory, NASA Marshall Space Flight Center, Huntsville, Alabama.
[2] Lockheed Martin Palo Alto Research Laboratory, Palo Alto, California.
[3] Rutherford Appleton Laboratory, Didcot, England, United Kingdom.
[4] Laboratory for Extraterrestrial Physics, Goddard Space Flight Center, Greenbelt, Maryland.
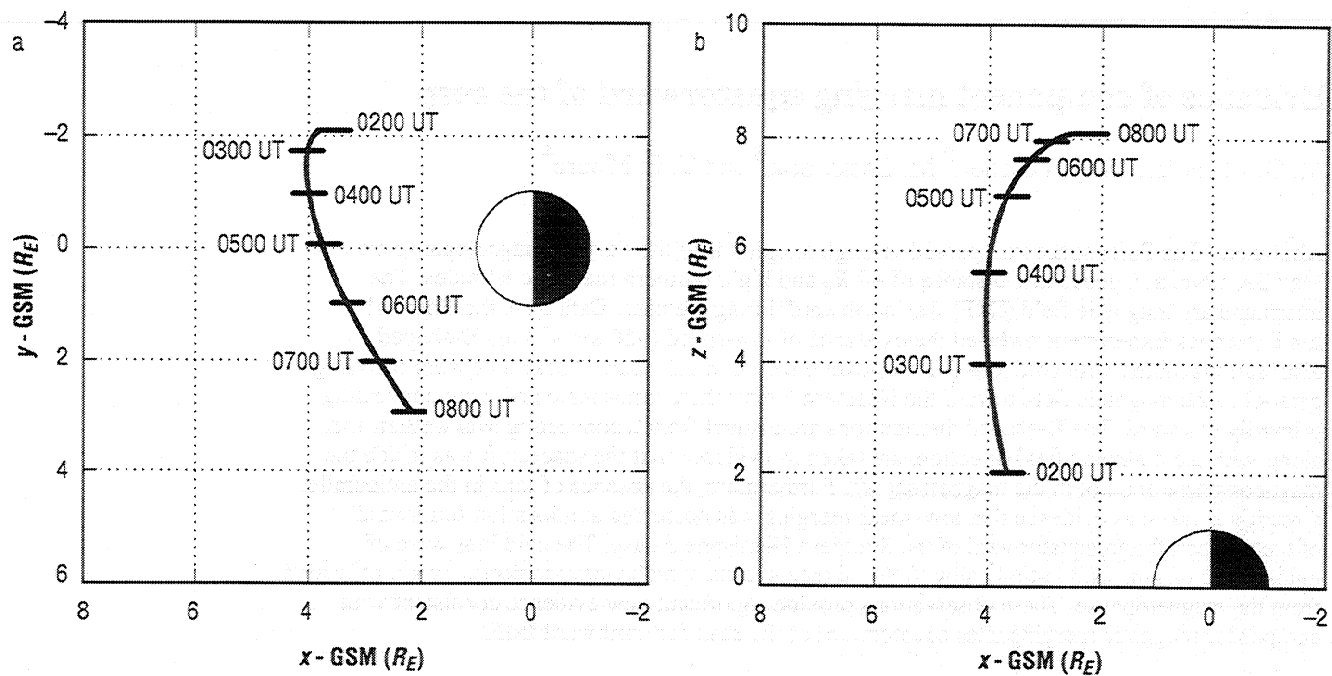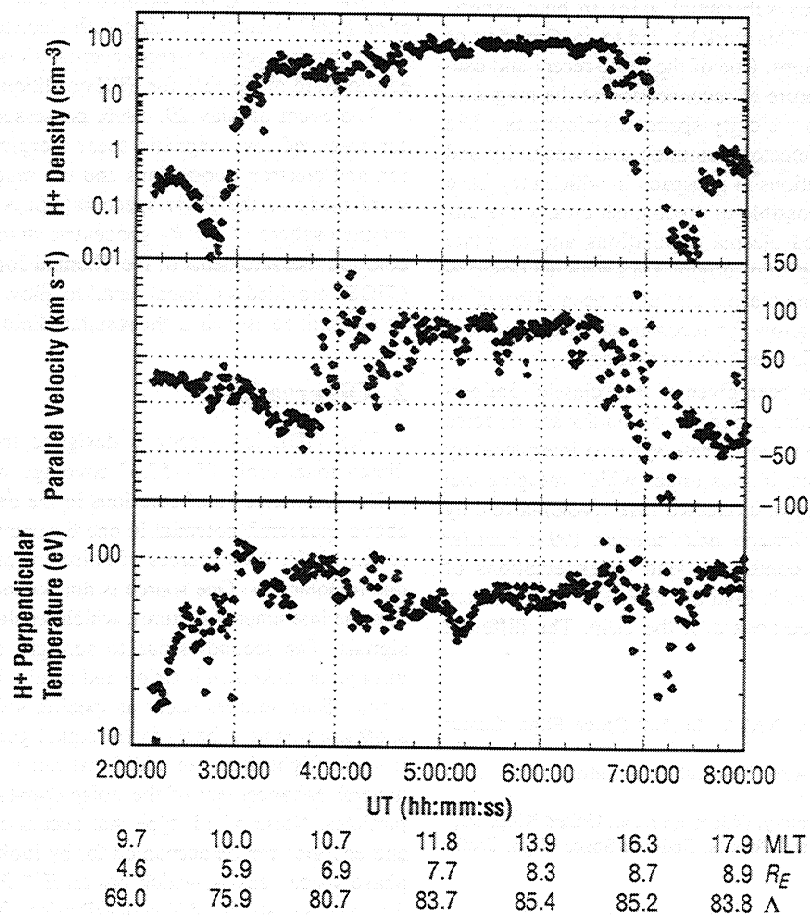
Figure 1. Polar trajectory in GSM (a) *x-y* plane and (b) *x-z* plane.

Figure 2. H$^+$ velocity moments for May 29, 1996, based on 1 min averages.

Plate 1. H$^+$ phase space density in a plane containing the local magnetic field (x direction) for 0540–0600 UT. The velocities are referenced to an Earth-fixed system with the origin denoted by the white cross. The black cross denoting the spacecraft velocity overwrites the white cross because of the low spacecraft speed.
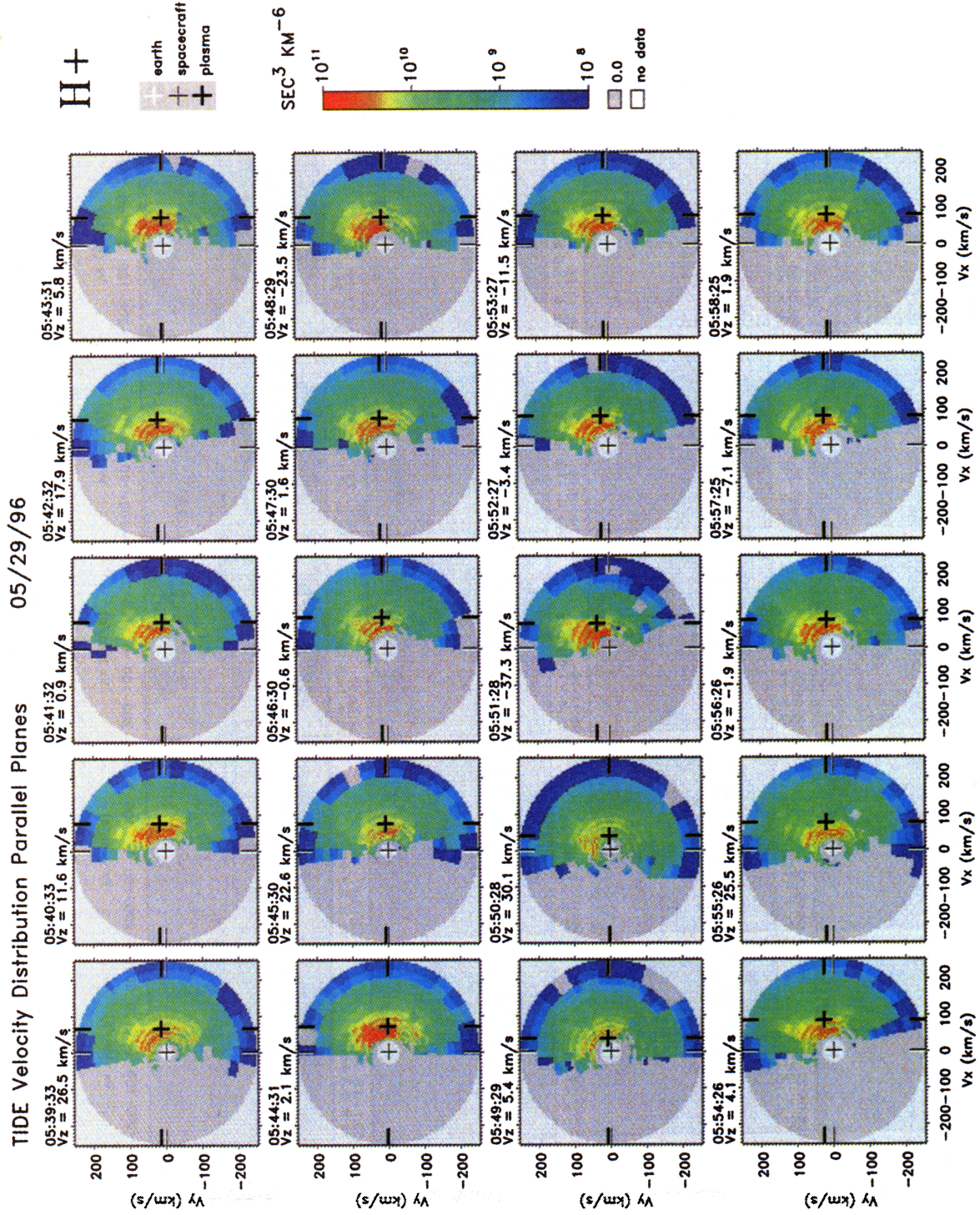
Plate 2. H+ phase space density in a plane containing the local magnetic field (x direction) for 0600–0520 UT. The velocities are referenced to an Earth-fixed system with the origin denoted by the white cross. The black cross denoting the spacecraft velocity overwrites the white cross because of the low spacecraft speed.
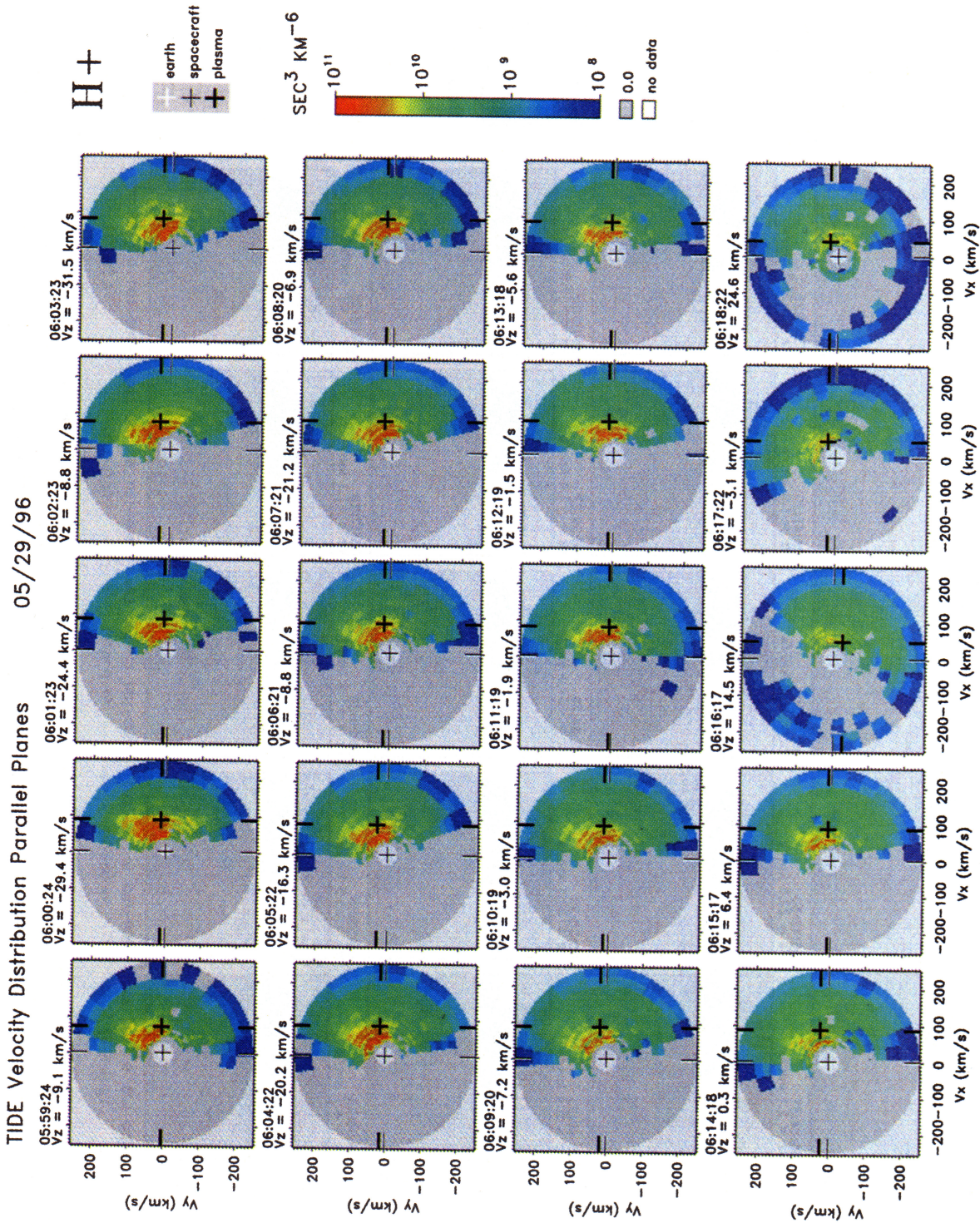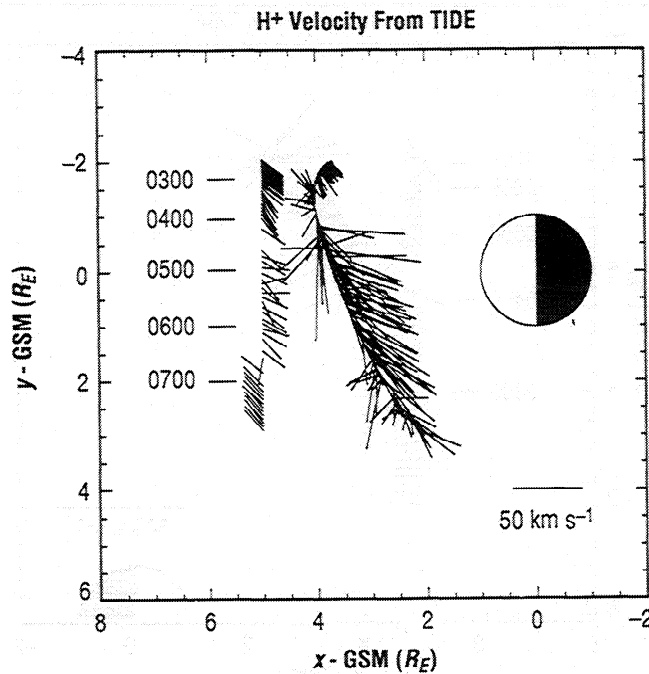
H+ Velocity From TIDE

Figure 3. H$^+$ velocities and the direction of the local magnetic field in the GSM x-y plane for May 29, 1996, 0230–0800 UT (1 min average). The ion velocities (plotted on the right) are referenced to the satellite track. The magnetic field direction is plotted as unit vectors with their tails anchored at $x = 5$.

were averaged (giving ~60 s time resolution), and n was determined to be 0.25. This corresponds to an assumption that an average is significant if more than four total counts were recorded during the averaging interval.

The TIDE data from the period from 0300 to 0800 UT have been reduced to two-dimensional and one-dimensional slices in phase space, and in addition, velocity moments were computed. During this period the Polar spacecraft traversed the dayside magnetosphere moving northward and eastward from ~1000 to ~1600 magnetic local time (MLT). At ~0400 UT, Polar entered a region of high-density (order of 10–100 cm^{-3}) ions and low magnetic field strength (Figure 1). It continued in this environment until ~0700 UT. The core ions, as characterized by the velocity moments of the TIDE data, had ~50 eV of thermal energy and a field-aligned speed of ~50 km s^{-1} (Figure 2).

The velocity, when viewed in two-dimensional projections in GSM coordinates (Figures 3–6) shows several distinct regions of plasma convection. Between 0300 and 0316 UT the convection was primarily sunward (Figures 5 and 6), consistent with convection toward the magnetopause. The plasma on these field lines exhibited the characteristic V shape associated with cusp ion injections from a distant site [cf. *Burch et al.*, 1982]. Near 0415 UT, another boundary was crossed, and the ions were observed to be moving northward, antisunward, and duskward. This is the approximate direction of the local magnetic field, but the ions in this region had a higher field-aligned speed than convection speed. The convection velocity was predominantly antisunward but toward the dawn side.

The primary focus of this paper is on the region starting near 0415 UT and ending near 0645 UT. In this period the flow veloc-

ity was predominantly field-aligned, and the magnetic field orientation was northward and tailward (Figure 4). Ion distributions from this period show a distinct D-shaped character [*Cowley*, 1982], which actually begins near 0340 UT but is persistent from 0440 to 0645 UT. Plates 1 and 2 show the phase space density for a two-dimensional slice in velocity space, which contains the local magnetic field. In these distributions a cross marks the flow velocity. The D shape is distinct with the flux parallel to **B** at least an order of magnitude higher than the flux antiparallel to **B**. The D shape is also persistent throughout Plates 1 and 2. The only distributions that do not exhibit this character are around 0510–0511 UT, where the distribution becomes more isotropic and the parallel velocity decreases to near zero.

One-dimensional cuts through these distributions (parallel to the local magnetic field) show additional structure not evident in the previous views (Figures 7–10). In order to make this data more quantitative it was necessary to reduce further the noise levels. Prior to this point a noise subtraction was performed that primarily removed the effects of sunlight entering the instrument. This also removed some of the instrumental noise. The final step included a removal of data below a constant n-count level. Two points are clear from this data. First, the nature of these low-energy ions is highly variable, showing significant changes on the shortest observable timescale of 6 s. In the final analysis, 60 s (or 10 satellite spin periods) averages were used to provide better significance in the phase space values. Second, beginning at ~0440 UT, the majority of the distributions are combinations of two populations. For example, Figure 8 shows a 60 s average from 0507 to 0508 UT that exhibits a prominent, narrow feature near 60 km s^{-1} superposed on the broader distribution. Using a
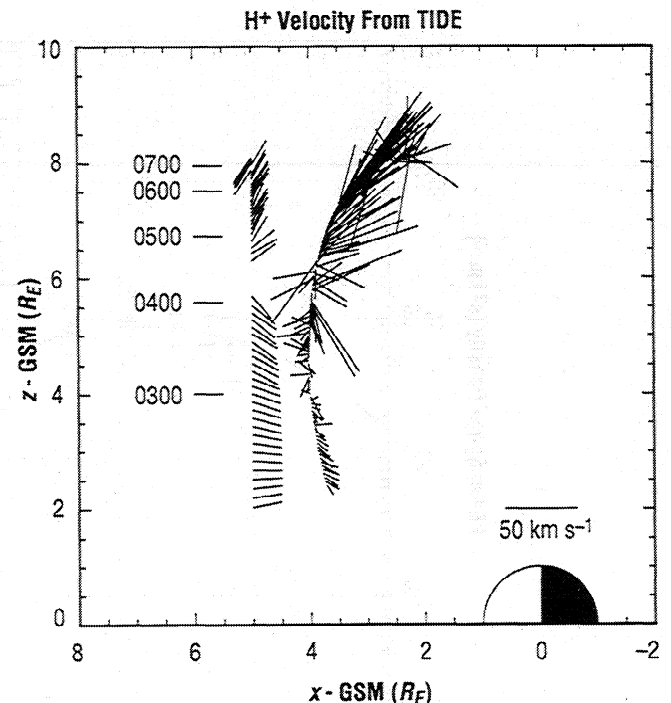
H+ Velocity From TIDE

Figure 4. H$^+$ velocities and the direction of the local magnetic field in the GSM x-z plane for May 29, 1996, 0230–0800 UT (1 min average). The ion velocities (plotted on the right) are referenced to the satellite track. The magnetic field direction is plotted as unit vectors with their tails anchored at $x = 5$.
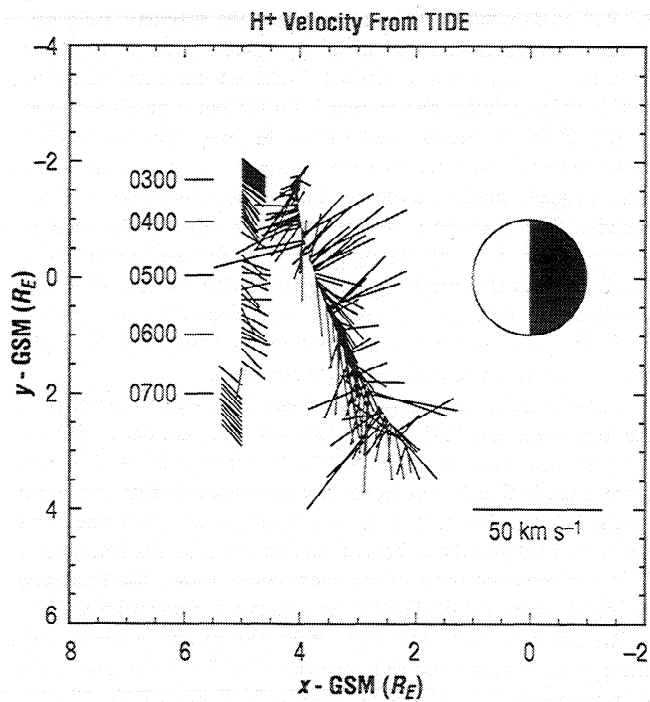
Figure 5. H⁺ velocities perpendicular to the local magnetic field and the direction of the local magnetic field in the GSM x-y plane for May 29, 1996, 0230–0800 UT (1 min average). The ion velocities (plotted on the right) are referenced to the satellite track. The magnetic field direction is plotted as unit vectors with their tails anchored at $x = 5$.

Figure 6. H⁺ velocities perpendicular to the local magnetic field and the direction of the local magnetic field in the GSM x-z plane for May 29, 1996, 0230–0800 UT (1 min average). The ion velocities (plotted on the right) are referenced to the satellite track. The magnetic field direction is plotted as unit vectors with their tails anchored at $x = 5$.
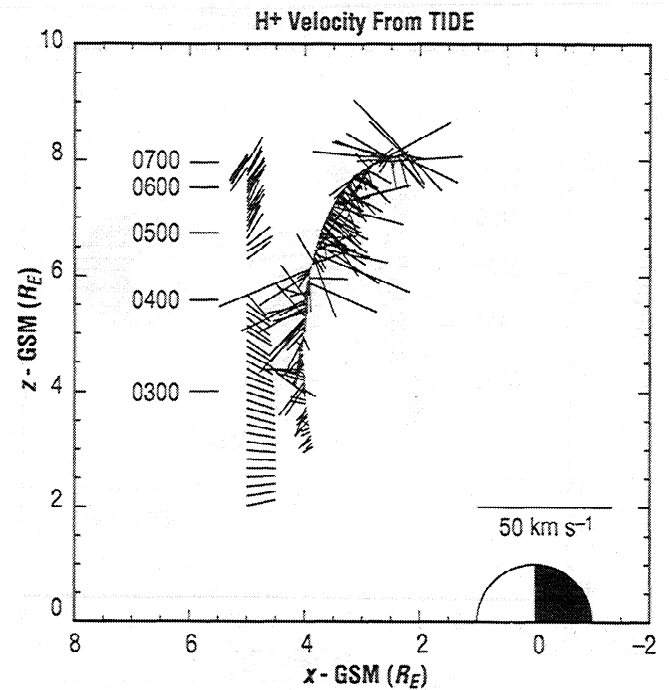

Figure 7. H⁺ velocity distribution for May 29, 1996, at 0436 UT (1 min average). The circles are the phase space densities in the direction parallel to the local magnetic field with associated error bars. The dashed curve is a best fit Maxwellian distribution with parameters as shown.

Figure 8. H$^+$ velocity distribution for May 29, 1996, at 0507 UT (1 min average). The circles are the phase space densities in the direction parallel to the local magnetic field with associated error bars. The dashed curves are best fit Maxwellian distributions representing the ionospheric population and the magnetosheath population with parameters as shown.
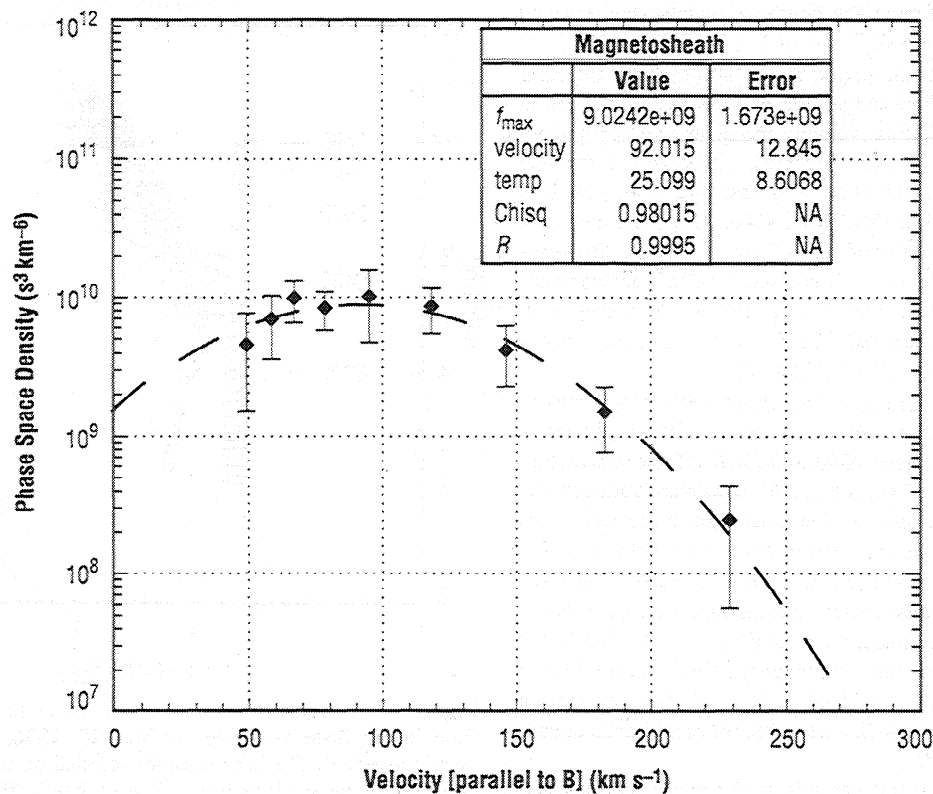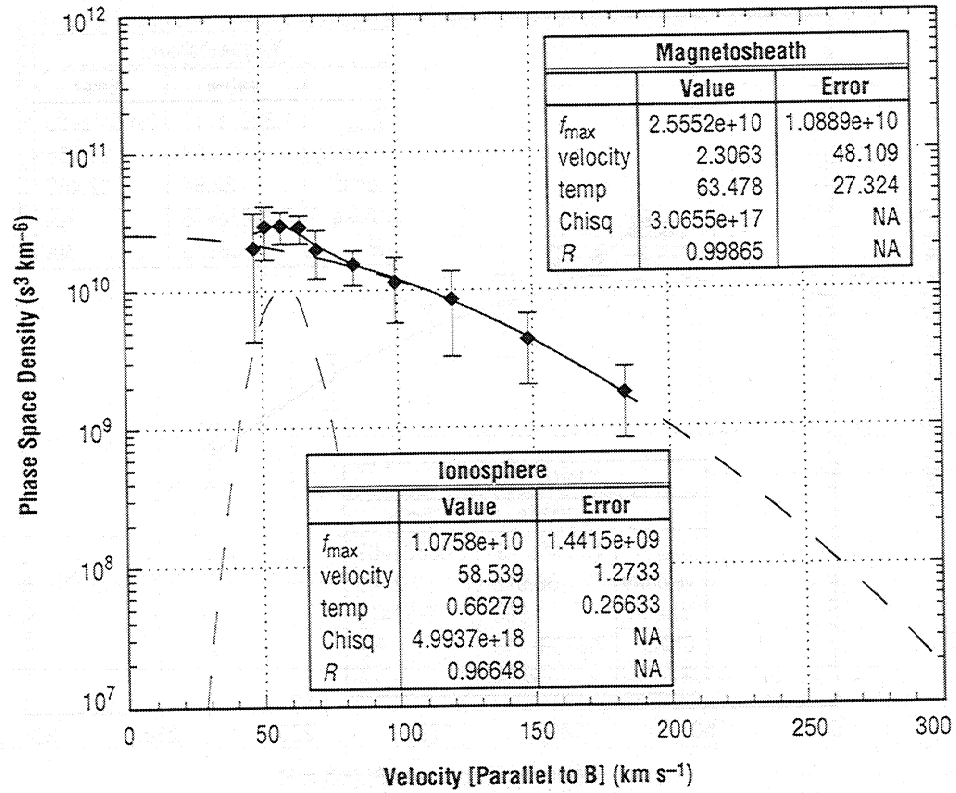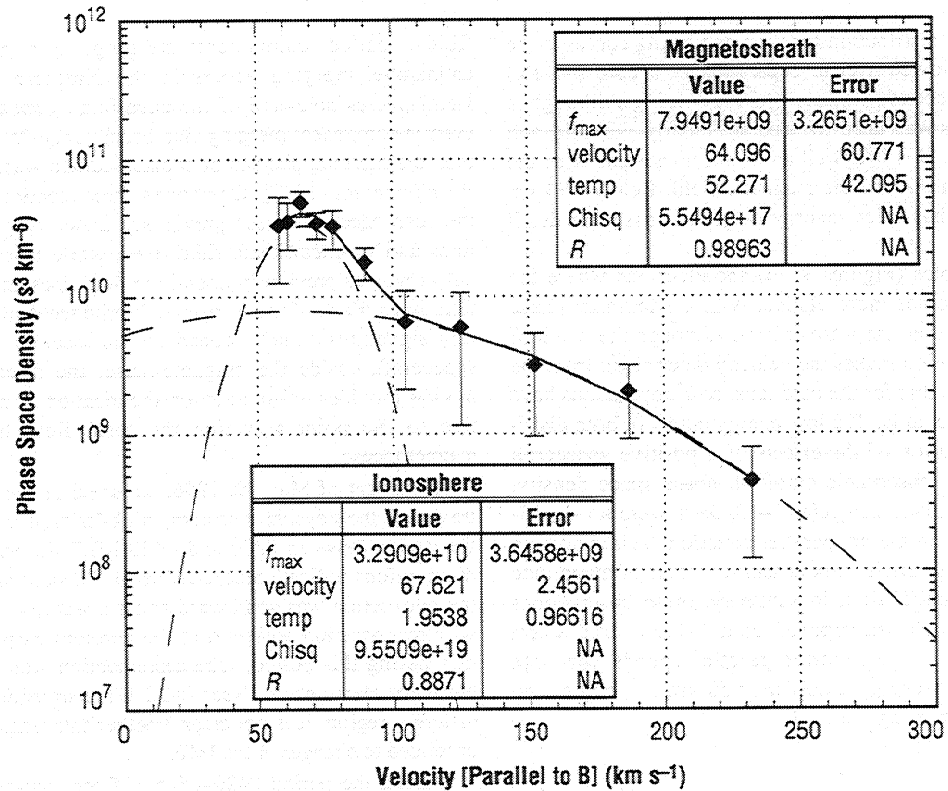

Figure 9. H$^+$ velocity distribution for May 29, 1996, at 0520 UT (1 min average). The circles are the phase space densities in the direction parallel to the local magnetic field with associated error bars. The dashed curves are best fit Maxwellian distributions representing the ionospheric population and the magnetosheath population with parameters as shown.

Figure 10. H$^+$ velocity distribution for May 29, 1996, at 0530 UT (1 min average). The circles are the phase space densities in the direction parallel to the local magnetic field with associated error bars. The dashed curves are best fit Maxwellian distributions representing the ionospheric population and the magnetosheath population with parameters as shown.
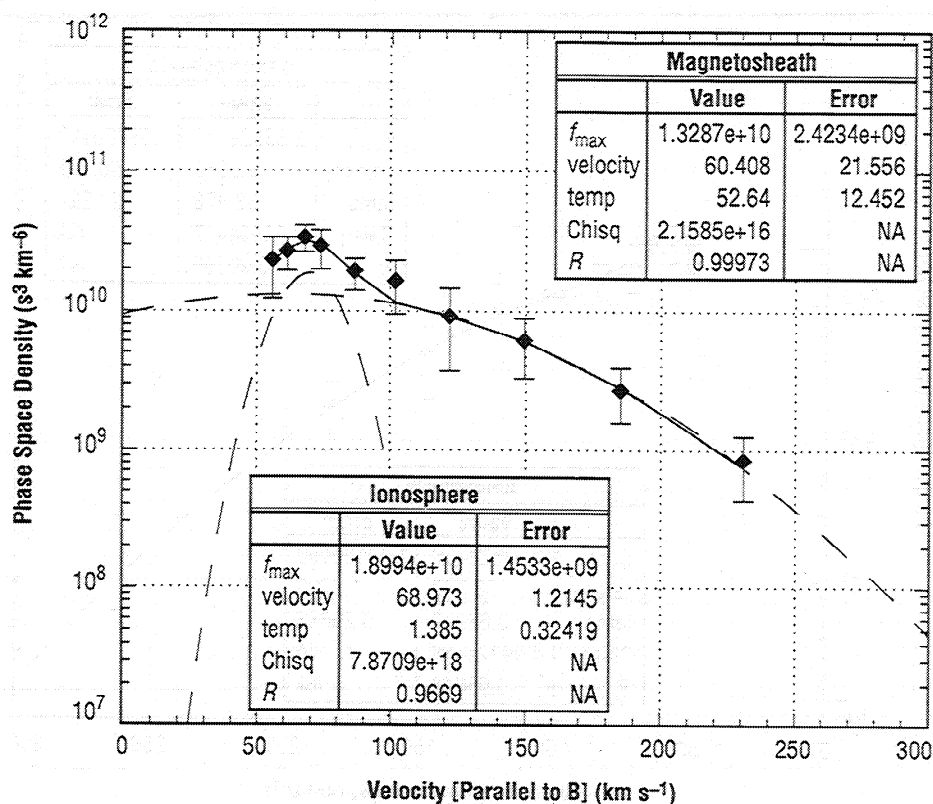
drifting, Maxwellian distribution function and fitting curves to the total distribution allowed a clear separation of a cold (~1 eV) population and a second, warmer (~60 eV) one. Although a drifting Maxwellian was used to separate clearly the cold and warmer populations, this Maxwellian is not consistent with the flux observed antiparallel to the magnetic field. Below ~50 km s^{-1} the distribution has a low-energy cutoff discussed in detail below.

Additional examples (Figures 9–10) show periods where the cold population becomes more distinct with a maximum phase space density higher than the warmer ions. Although the width of the warm ion distribution makes the velocity determined from the fits less accurate than that for the cold ions, both populations have similar speeds parallel to **B**. The low-energy cutoff in both distributions is a combination of the effects of a positive spacecraft potential and a true, observable cutoff in phase space density. During the periods shown in Figures 7–10, there were no significant counts observed in the antiparallel direction. This places an upper limit on the antiparallel flux at least an order of magnitude below that of the parallel flux. In summary, these observations are characterized by (1) superposed cold (~1 eV) and warm (~50 eV) populations, (2) similar parallel speeds for both populations, (3) a low-energy cutoff near 50 km s^{-1}, and (4) no observable counterstreaming ions.

3. Discussion

There are two principal types of magnetic merging. One type is merging between strictly antiparallel fields, called antiparallel merging, and the other type is merging between nonparallel fields, called component merging. For northward IMF, antiparallel merging occurs in the Northern and/or Southern Hemispheres poleward of the cusp [e.g., *Crooker*, 1979]. However, if component merging also occurs under this IMF condition, then the merging site can be located equatorward of the cusp [cf. *Fuselier et al.*, 1997]. Component reconnection equatorward of the cusp occurs between previously closed magnetospheric field lines and magnetosheath field lines, while that poleward of the cusp involves previously open-lobe field lines and magnetosheath field lines. Each of these cases will produce distinct ion and electron signatures, which depend on the location of the observing spacecraft. Inside the magnetopause, the direction of the ion motion provides information on the location of the observer relative to the point at which the local field line crossed the magnetopause.

The event of May 29, 1996, occurred as the Polar spacecraft traversed the dayside, northern, high-latitude magnetosphere. In the period between 0300 and 0420 MLT the velocity-filtered V distributions indicate reconnection at a distant site. Furthermore, the convection was southward and sunward, which is consistent with reconnection poleward of the northern cusp. Thus it appears that during this period, lobe reconnection was occurring in the Northern Hemisphere. Near 0420 UT a transition occurred to a different region. It is not clear whether this transition was spatial or related to changes in the IMF.

During the period 0420–0645 UT the low-energy ion signatures can be summarized as (1) superposed cold (~1 eV) and warm (~50 eV) populations, (2) similar parallel speeds for both populations, (3) a low-energy cutoff near 50 km s^{-1}, and (4) no observable counterstreaming ions.
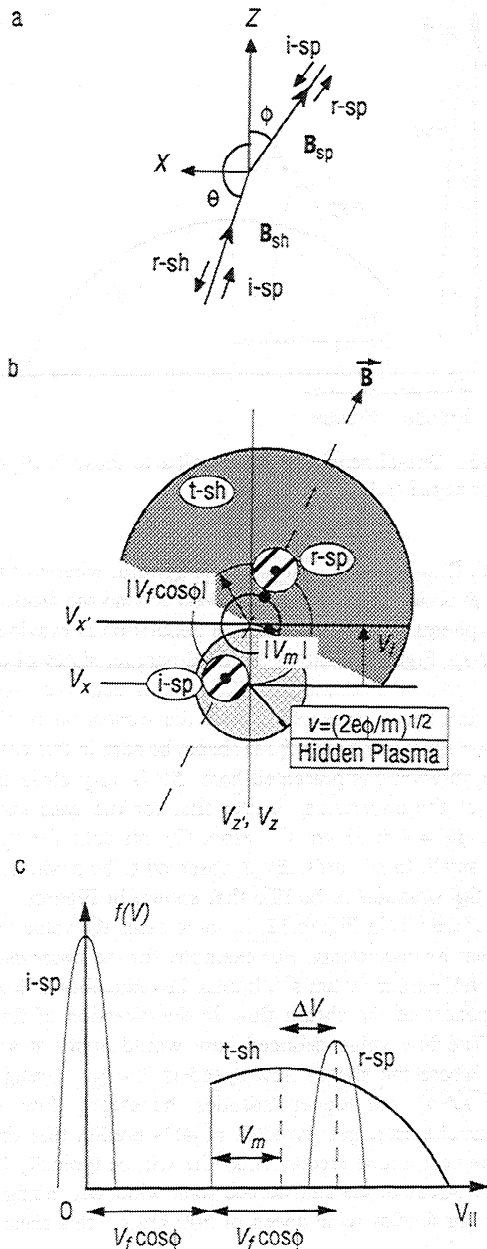
Figure 11. (a) Possible ion components for northward directed V_f. (b) Expected phase space density signatures for northward directed V_f. (c) One-dimensional cuts through distribution in Figure 11b.

Cowley [1982] outlined the different signatures expected inside and outside the magnetopause. Generalizing that work, Figure 11a shows the ion populations incident on, reflected by, and transmitted through the magnetopause rotational discontinuity for northward IMF Bz. The z direction lies in the plane of the magnetopause and points in the direction of V_f, the field line velocity over the magnetopause (the de Hoffman-Teller velocity), and the x direction is the outward normal to the magnetopause: θ and φ are the angles that the projection of the magnetic field onto the zx plane make with the magnetopause in the magnetosheath and in the open low-latitude boundary layer (LLBL), respectively. The i-sh population comprises magnetosheath ions incident on the magnetopause, which is reflected to give the r-sh or transmitted into the magnetosphere to give the t-sh. Similarly,

the i-sp population comprises the magnetospheric ions incident on the boundary, which are reflected or transmitted to give r-sp and t-sp, respectively. Here the primary concentration is on the sp ions, which are of ionospheric origin.

The magnetosheath-like population observed by TIDE has a low-velocity cutoff giving the D-shaped distribution of the type predicted by *Cowley* [1982] and observed in data from close to the magnetopause [*Fuselier et al.*, 1991; *Smith and Rodgers*, 1991; *Gosling et al.*, 1991]. This population could be either i-sh or t-sh. For it to be the incident population i-sh, there must be undetectable reflected ions, r-sh, i.e., the reflection coefficient r is very small. This is not consistent with the observations of *Fuselier et al.* [1991], who showed r was near the 0.5. However, if magnetospheric densities were very low, r would tend to zero. The incident population in the magnetosheath boundary layer has a D-shaped distribution function because sheath ions cannot flow out of the magnetosphere. The only exception to this would be if the field line had been open sufficiently long for injected sheath ions to mirror at low altitudes and return to the spacecraft. The sheath-like population observed could not be the reflected sheath ion r-sh since the incident population would also have been observed.

Consider the ionospheric populations for these two possibilities. If the sheath-like ions are i-sh (with small r and no mirrored ions), then the ionospheric population present would have to be part of the transmitted t-sp population and would therefore be accelerated by crossing the magnetopause (as is the case for the observed ionospheric component presented here.) However, these ions would be moving in the opposite direction to the sheath ions, which is not the case, thus eliminating this possibility.

The other possibility is that the observed t-sh population is in the open LLBL. In this case, two ionospheric populations would be present. The incident i-sp ions would be unaccelerated and would not be detected above the low-energy threshold of the instrument set by the positive spacecraft potential. The reflected r-sp ions would be accelerated and moving in the same direction as the sheath ions. Therefore this possibility is the only one that agrees with the observations.

The similarity of the bulk flow speed of the ionospheric and magnetosheath ions indicates that the magnetosheath flow speed was low at the point where these ions crossed the magnetopause (in other words, that point was close to the subsolar region). To make this argument, we need to generalize the construction that *Cowley* [1982] used to allow for magnetosheath flow. Cowley assumed that all the incident populations (i-sh and i-sp) had no field-parallel flow. Although this assumption is good for the low-energy ionospheric ions, it is not good for the sheath ions because of the magnetosheath flow away from the subsolar point. Figure 11b shows the construction of Cowley but generalized for a nonzero boundary-tangential sheath flow. The component of this flow in the z direction is V_{sh} and is defined as positive in the same direction as the field line motion, V_f. Figure 11b is a velocity-space plot in the zx frame, with O being the origin in the Earth's frame of reference and O' being the origin in the de Hoffman-Teller frame. The dots give the peaks of the distribution function f (approximately the same as the bulk flow velocity) for the incident and transmitted sheath ion populations (i-sh and t-sh). The shaded regions show the populations where $f(v)$ exceeds an arbitrary threshold value and reveals the D-shape of the distributions. Also shown are the peaks of the incident and reflected ionospheric populations (i-sp and r-sp), the dark shaded regions for these populations being smaller because of their low temperature. In the de Hoffman-Teller frame, there is no electric
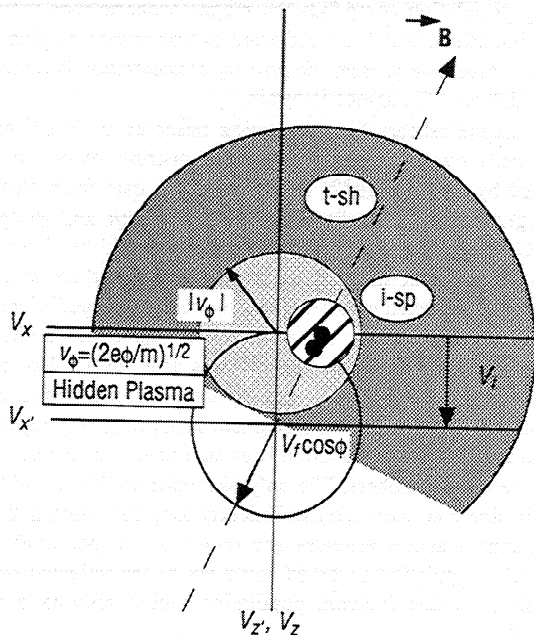
Figure 12. Expected phase space density signatures for southward directed V_f.

Figure 13. One-dimensional cuts similar to those in Figure 11b except for negative Δv.

field, and so, the peaks of the distributions remain at the same velocity, i.e., they remain on the circles given as dotted lines. These circles have radius $V_f \cos \phi$ and V_m. Note that the i-sp ions have no field-parallel velocity but are convecting toward the magnetopause under the influence of the boundary tangential electric field. In the Earth's frame the i-sp population peak has zero field-aligned velocity, but the r-sp population has a peak at $2V_f \cos \phi$, as predicted by *Cowley* [1982]. In the case of the sheath ions the magnetosheath flow means that the peak of the distribution function is at a speed V_m in the de Hoffman-Teller frame and from Figure 11b

$$V_m \cos\theta + V_{sh} = V_f \qquad (1)$$

In the Earth's frame the peak of the transmitted population is at a field-aligned velocity of $(V_f \cos \phi + V_m)$. Therefore the difference in the field-aligned flow velocities in the Earth's frame of the r-sp and t-sh populations is, by (1),

$$\begin{aligned} \Delta V &= 2V_f \cos \phi - (V_f \cos \phi + V_m) \\ &= [(V_f (\cos \phi \cos\theta - 1) + V_{sh}] / \cos\theta \end{aligned} \qquad (2)$$

In cases where ϕ and θ are small, so $\cos \phi \approx \cos\theta \approx 1$, ΔV is equal to V_{sh}. Note that ΔV is defined as positive when the bulk flow of the r-sp population exceeds that of the t-sh.

Figure 11b shows the situation when $V_{sh} > 0$. This applies at locations away from the subsolar point at times when reconnection is near the subsolar point. In this case, as the field line evolves away from the reconnection site, both the field line motion and the magnetosheath flow are antisunward, making the component of the sheath flow in the direction of field line motion (V_{sh}) positive. In this case, ΔV is positive. Figure 11c shows the field-parallel slices of the distribution functions in this case. Note that for locations close to the subsolar point, both ΔV and V_{sh} tend to zero.

Figure 12 shows the corresponding situation for $V_{sh} < 0$, which would apply sunward of a lobe reconnection site. In such cases
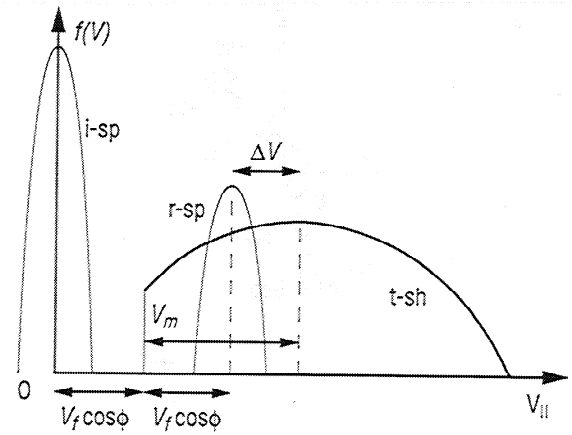
the sheath flow is significant and antisunward, whereas the field lines are evolving sunward (or east/west around the flanks of the magnetosphere). In this case the t-sh population is moving faster that the r-sp. Figure 13 shows the field-parallel slices of the distributions, and in this case, ΔV, like V_{sh}, is negative. Note that only at very low values of $f(v)$ can the truncation of the t-sh distribution function (giving the D shape) be seen in this case.

In the observations presented here, ΔV is very close to zero. Because of the uncertainty in the fits, for the case shown in Figure 9, $\Delta V = 4 \pm 63$ km s^{-1}. From (2) this calls for V_{sh} to be similarly small. In all cases, ΔV is observed to be positive, which requires the situation to be like that shown in Figures 11b and 11c, rather than as in Figure 12. In some cases the value of ΔV is larger than the uncertainty. For example, for the observations in Figure 8, $\Delta V = 56 \pm 49$ km s^{-1}. It must be remembered that V_{sh} is the component of the sheath flow in the direction of field line motion. The low value deduced here would apply at subsolar latitudes where the sheath flow speed is low [cf. *Onsager and Fuselier*, 1994]. For higher latitudes the sheath flow will be faster. For example, gas dynamic models predict that the flow magnitude near a lobe reconnection site will be typically 0.6–0.9 of the flow speed of the undisturbed solar wind, depending on the location. For a solar wind speed of 500 km s^{-1} this sheath flow

View From Dawn

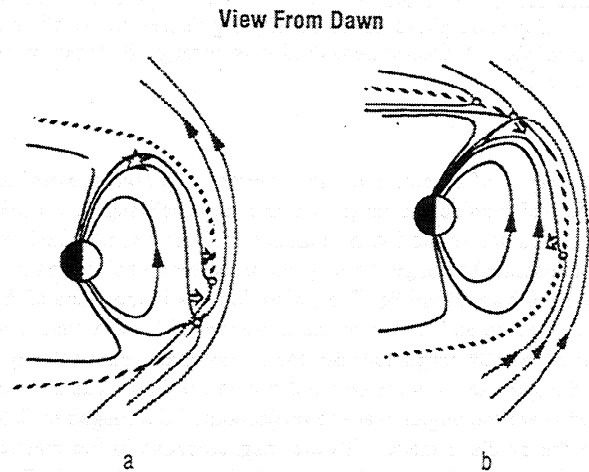a   b

Figure 14. Field line topology and motion for two cases of component merging. (The star indicates the general location of Polar spacecraft during observations.)

speed will be of order 300–450 km s^{-1}. Therefore the only way that V_{sh} could have the low-value magnitude (<60 km s^{-1}) deduced here for a lobe reconnection site is if the reconnected field lines are evolving in a direction that is very close (within ~8°) to perpendicular to the local sheath flow direction. This requires a rather special set of circumstances and fixes the magnitude and direction of the tension force required. On the contrary, the situation with small values of ΔV was observed over an extended period of time.

The peak of the ionospheric ion distribution shows that $2V_f$ cos ϕ is of order 60 km s^{-1}, which yields $V_f > 30$ km s^{-1}. This field line motion at the magnetopause is consistent with the low-energy cutoff of both distributions (at V_f cos ϕ), which were seen to be between zero and 50 km s^{-1}. This positive value for V_f means that the point where the field line crosses the magnetopause is moving in such a way as to shorten the field line, i.e., generally antisunward in the case of low-latitude reconnection or sunward in the case of lobe reconnection. Without such motion, acceleration in the Earth's frame would not be found. For all locations on the lobe boundary the sheath flow would be in a direction to move the field line antisunward, giving a large component of the flow that is antiparallel to the V_f inferred here. During the times when the mixed population was observed the E×B drift velocity of the plasma at the satellite was typically 20 km s^{-1} and primarily in the +Y direction (i.e., around the afternoon sector toward dusk) with a smaller component in the −X and −Z directions (Figures 5 and 6). This is consistent with antisunward convection away from a low-latitude reconnection site, with field lines moving under sheath flow with some influence of the magnetic tension force, for a weakly positive IMF B$_y$ component. (Lagged data from the Wind satellite show that B$_y$ was indeed mainly positive, fluctuating between ~0 and +5 nT during this interval.) For such convection to be shortening a reconnected field line the reconnection must have taken place at low latitudes. From the above it is concluded that the lobe reconnection hypothesis is not credible and that the Polar/TIDE observations were of particle entry through the low-latitude magnetopause as illustrated qualitatively in Figure 14.

4. Conclusions

The evidence obtained from the TIDE ion observations confirm that the Polar spacecraft passed through a region near the northern magnetic cusp, which was threaded by field lines connected to the solar wind. The existence of low-speed (~50 km s^{-1}) ion D-shaped distributions mixed with cold ions (~2 eV) traveling parallel to the magnetic field in the absence of ions in the antiparallel direction is taken as evidence that low shear merging was occurring at a location southward of the spacecraft and equatorward of the Southern Hemisphere cusp. The cold ions were of ionospheric origin, with initially slow field-aligned speeds, which were accelerated upon reflection from the magnetopause. The absence of low-speed cold ions in the observations is due to a several-volt positive spacecraft potential. These observations provide significant new evidence consistent with magnetic merging sites equatorward of the cusps for northward IMF.

References

Burch, J. L., P. H. Reiff, R. A. Heelis, J. D. Winningham, W. B. Hanson, C. Gurgiolo, J. D. Menietti, R. A. Hoffman, and J. N. Barfield, Plasma injection and transport in the mid-altitude polar cusp, *Geophys. Res. Lett.*, 9, 921, 1982.

Cowley, S. H. W., The causes of convection in the Earth's magnetosphere: A review of developments during the IMS, *Rev. Geophys.*, 20, 531, 1982.

Crooker, N. U., Dayside merging and cusp geometry, *J. Geophys. Res.*, 84, 951, 1979.

Dungey, J. W., Inteplanetary field and the auroral zones, *Phys. Rev. Lett.*, 6, 47, 1961.

Fuselier, S. A., D. M. Klumpar, and E. G. Shelley, Ion reflection and transmission during reconnection at the Earth's subsolar magnetopause, *Geophys. Res. Lett.*, 18, 139, 1991.

Fuselier, S. A., B. J. Anderson, and T. G. Onsager, Particle signatures of magnetic topology at the magnetopause: AMPTE/CCE observations, *J. Geophys. Res.*, 100, 11,805, 1995.

Fuselier, S. A., B. J. Anderson, and T. G. Onsager, Electron and ion signatures of field line topology at the low-shear magnetopause, *J. Geophys. Res.*, 102, 4847, 1997.

Gosling, J. T., M. F. Thomsen, S. J. Bame, R. C. Elphic, and C. T. Russell, Observations of reconnection of inteplanetary and lobe magnetic field lines at the high-latitude magnetopause, *J. Geophys. Res.*, 96, 14,097, 1991.

Moore, T. E., et al., The Thermal Ion Dynamics Experiment and Plasma Source Instrument, *Space Sci. Rev.*, 71, 409, 1995.

Onsager, T. G., and S. A. Fuselier, The location of magnetopause reconnection for northward and southward interplanetary field, in *Solar System Plasmas in Space and Time*, Geophys. Monogr. Ser., Vol. 84, edited by J. Burch and J. W. Waite, p. 183, AGU, Washington, D. C., 1994.

Smith, M. F., and D. J. Rodgers, Ion distributions at the dayside magnetopause, *J. Geophys. Res.*, 96, 11,617, 1991.

M. O. Chandler, Space Sciences Laboratory, NASA Marshall Space Flight Center, MS ES–83, Huntsville, AL 35812. (Michael.Chandler@msfc.nasa.gov)

S. A. Fuselier, Lockheed Martin Palo Alto Research Laboratory, Palo Alto, CA 94304-1187.

M. Lockwood, Rutherford Appleton Laboratory, Didcot, England, United Kingdom OX11 0QX.

T. E. Moore, Laboratory for Extraterrestrial Physics, Goddard Space Flight Center, Greenbelt, MD 20771.